Probabilistic Model of AFDX Frames Reception for End System Backlog Assessment

Yohan Baga*†, Morgane Richaud*, Fakhreddine Ghaffari*, Etienne Zante†, David Declercq* and Michael Nahmiyace†
*ETIS, UMR 8051 / ENSEA, University of Cergy-Pontoise, CNRS, F-95000, Cergy-Pontoise, France
Email: (yohan.baga, morgane.richaud, fakhreddine.ghaffari, david.declercq)@ensea.fr
†ZODIAC AEROSPACE, Zodiac Aero Electric, Zodiac Cockpit and Lighting Systems, Montreuil, France
Email: etienne.zante@zodiacaerospace.com

***Abstract*—The Avionics Full-Duplex Switched Ethernet (AFDX) network has established itself as a reference in aeronautical embedded communications to comply with the growth of bandwidth needs and the reliability requirements. Its determinism property imposes that AFDX frames have to transit through the network in a limited amount of time. Due to potential delays in the processing frames at a reception End-System, the frames have to be stored in a reception buffer. Generally, the buffer is dimensioned enough large to avoid prohibitive frame losses, but it results a waste of memory resources.**

The buffer dimensioning issue requires an analysis of the reception flow to determine the worst frame backlog. As the frame backlog is maximal when a sequence of back-to-back frames is received by the ES, the key point is to estimate the occurrences of such SBFs on a representative sample of received frames. In this paper, we address this issue using a probabilistic model based on local Gaussian distributions, and we propose results for a range of typical configuration tables of the reception End-System.

Keywords **–** AFDX, Avionics network, Back-to-back Frames, End-System Reception Buffer, Probabilistic Distribution, Reception Flow

I. Introduction

The exacerbation of safety rules and requirements of the airlines leads the aircraft manufacturers to develop increasingly efficient and complex embedded technologies disseminated on-board. The hardware and software sensors, data processing units and actuators (End-Systems) have to be correctly deployed and connected through a reliable and high speed network. As the technology complexity is growing, the communication medium as well as the frames processing in the End-Systems become a critical issue in terms of available bandwidth, reliability, determinism and certification.

Since its successful implementation in the Airbus A380, the AFDX network based on the mature Ethernet protocol has been widely adopted as a good candidate to meet requirements of embedded communications. AFDX [1] presents significant improvements compared to older communication standards [2], [3], in particular, in terms of available bandwidth and reliability thanks to enforcement of redundancy mechanisms. Moreover, determinism is guaranteed both by the segregation of source flows (Virtual Links), and by traffic regulation mechanisms in the source ESs (Bandwidth Allocation Gap). The determinism is proven by the existence of end-to-end delays for the transit of frames onto the virtual links using methods like approved Network Calculus [4], recent Trajectory Approach [5] or Forward End-to-End delays Analysis [6].

978-1-5386-3166-9/17/$31.00

Depending on the static network configuration, an ES receives frames from one or several other ESs which can lead to an loaded traffic in reception. The ES has to process AFDX received frames to extract data intended to hosted software applications of the equipment. However, delays can occur in the processing frames at the reception ES level which impose the use of a queuing reception buffer to store arriving to-be-processed frames. Considering the variability of the received frames flow due to network jitters and the overall asynchronous feature of the network, the buffer dimensioning becomes a critical issue both to avoid a prohibitive loss of frames, and to not overestimate the buffer size to avoid unused memory resources.

In previous work [7], we have presented a deterministic worst case method to find an upper bound for the backlog in the ES reception buffer, and we have evaluated the influence of several ES reception parameters on the worst backlog. Under a constant frame reading delay, we have highlighted that the backlog strongly depends on the input frames flow from AFDX network, in particular, when a sequence of back-to-back frames is received. Thus, we have justified that the longest sequence of back-to-back frames (LSBF) is the key to determine the worst frame backlog in the ES reception buffer.

In this paper, we propose a probabilistic approach that relies on the temporal characterization of the reception flow based on Gaussian distributions to evaluate the occurrences of back-to-back frames on a representative sample of frames. Under the assumption of a BAG-periodic transmission of frames on all VLs, the Gaussian distribution-based model allows to take into account the random feature of reception date because of the jitters or delays, and to consider that the probability for a frame to meet a congestion in switch output ports is variable as the physical paths of virtual channels can across a different number of switches before reaching the reception ES.

The rest of the paper is organized as follow. The AFDX network main features are introduced in Section II. Section III describes the Gaussian-distribution model and the required adaptations to model the reception flow. Section IV presents the test conditions, the simulation results and a comparison with previous works. Finally, the paper concludes in Section

V.

II. AFDX Network: main features

AFDX networks provide real-time and reliable transmission services to software applications due to both physical network elements like ESs and switches and a communication protocol based on temporal segregation through Virtual Links (VLs). In this section, we introduce an AFDX network overview, and especially the VL notion, the model of reception ESs and switches.

A. Network General Organization & Temporal Segregation

As shown on Fig. 1, an homogeneous AFDX network is organized around redundant connected switches which constitute the AFDX interconnects, and ESs which are the network sources and sinks. VLs are conceptual communication paths used to ensure deterministic data transmission and temporal isolation between one source ES towards one or several reception ES(s). Thus, several ESs can instantiate independent communications thanks to static-defined and reliable VLs. Various multicast or unicast VLs send frames onto unidirectional paths like for example $P_{1,5} = \{ES_1, Sw_1, Sw_3, Sw_5, ES_9\}$ for which ES_1 is the source ES, Sw_1, Sw_3, Sw_5 are the 3-crossed switches, and ES_9 is the reception ES.

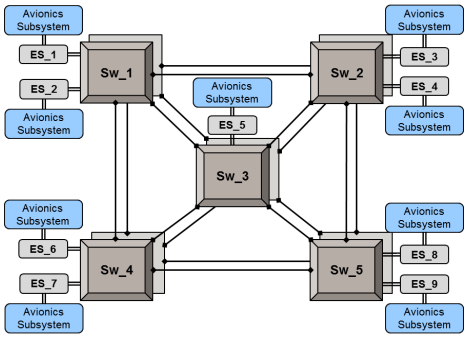

Fig. 1: AFDX Network Model with 5 Redundant Switches and 9 End-Systems.

In transmission, the Bandwidth Allocation Gap (BAG) constraints each VL by defining a minimal period between two consecutive transmissions on the same VL. Moreover, some jitters can occur during transmission because of concurrent frames access to the physical link. Some works [8], [9] deal with the jitter control and propose models to simulate and check the deterministic property while others tend to optimize the VL utilization using phase shifting [10] or proposing wise network topologies [11].

B. Reception End-System Architecture

The reception ES detects arriving frames and it realizes operations to extract the useful data from frames according to Ethernet-based protocol. Fig. 2 represents a model of a reception ES organized in layers with two active redundant networks. Network A and Network B transmit redundant frames to the MAC / PHY layer via the ARINC 600-compliant connectors. The MAC / PHY layer realizes the demultiplexing of frames and some checks about the frame length, the cyclic redundancy check or the destination address. Next, the Integrity Checking (IC) unit controls the sequence number of every frame, and then the Redundancy Management (RM) unit transmits the first valid frame to the ES reception FIFO memory and discards the other one. At any step, the CTRES provides static parameters to allow the checks correctness, in particular the BAG and the Maximal Frame Length (MFL).

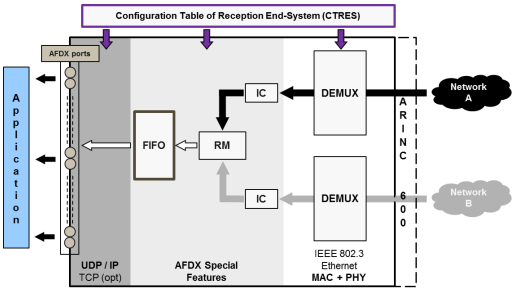

Fig. 2: Model of a Reception End-System with its 3 Processing Layers : MAC / PHY ; AFDX Special Features and UDP / IP.

The final and Ethernet-typical layer UDP / IP achieves a significant number of checks before delivering frame data to AFDX ports, and it may be the source of substantial delays and especially if these processes are led by software mechanisms. Therefore, the reception FIFO memory deserves a particular attention about dimensioning issue to avoid overflows or to waste memory resources with a too large buffer.

In [7], the LSBF leads to the Worst Frame Backlog (WFB) then used to optimize the size of the reception buffer. In this paper, we focus on the SBFs and we evaluate occurrences of such sequences with a probabilistic Gaussian distribution-based model of the reception flow. Finally, we compare the simulation results of the probabilistic model with results from the deterministic model, in order to estimate the relevance of the deterministic-based buffer dimensioning.

III. Modeling of the Frame Input Flow based on the Gaussian Distribution

In this section, we introduce the Gaussian-based model of the frames input flow. We carefully justify why it can be adapted to simply model the delay variations of frames transit from an analysis of the AFDX network behavior. For a given CTRES, our probabilistic model randomly builds sets of SBFs identified among several millions of received frames.

A. The Gaussian Distribution: Mathematical Model

Let's start by general properties about the Gaussian distribution, and why this distribution is adapted to model the input flow of frames at a reception ES. To respect with the determinism property, the overall load of the AFDX network is light. Consequently, a frame has more chances to be received after a transit duration equals to the minimal one computed with an empty network and so, without meeting any congestion

in the outputs of the switches. Moreover, the more we consider a distant date from the minimum date *Tmin* of arrival, the lower is the probability to receive the frame since this implies that switches congestion occurred and / or the frame undergone jitters. These two temporal phenomenons are intrinsically linked to the properties of the Gaussian distribution.

The Gaussian distribution is also the distribution with the maximum entropy among all the other existing distributions with a fixed variance. It means that the Gaussian distribution has the maximum randomness. This feature consolidates our proposal as the exact arrival date of any frame, even on the same VL, randomly varies during the network operations.

The mathematical expression of a Gaussian distribution is $N(\mu, \sigma^2)$ which depends on two parameters σ and μ and is defined by its density function in Eq. 1.

$$f_Y = \frac{1}{\sigma\sqrt{2\pi}} \times exp(-\frac{(y-\mu)^2}{2\sigma^2}) \quad (1)$$

The μ parameter is the mean of the distribution, that is to say it represents the central position of the distribution. The σ parameter is the standard deviation of the distribution and σ^2 the variance which is a dispersion metric.

B. Application of the Gaussian Distribution to the AFDX Input Flow

In this part, we take advantage of the Gaussian distribution to model the input flow, and we set σ and μ parameters to adapt the distribution to AFDX constraints. We also expose the procedure to draw a large number of arrival frames dates.

1) Implementation of the Gaussian Distribution as Algorithm: To interpret the fact that the highest probability to receive a frame is close to *Tmin*, we set μ to zero and we only consider the positive part of the Gaussian distribution. The σ parameter accounts for the delays that a frame could meet on the network. If a VL passes through several switches, it has more chances to meet at least one congestion. Therefore, a VL has a higher σ parameter when it passes through 2 switches than 1 switch for example. As each VL of the CTRES can have different ES sources and so, different physical paths of the network, it appears that each VL needs an individual σ parameter depending on the number of switches it crosses. In our model, we will consider a VL can pass through a maximum of 3 switches for a sake of simplicity but the model could easily be extended to more switches. Thus, we fix three representative intervals of values for σ:

- $\sigma \in$] 0 ; 1] when the VL crosses 1 switch;
- $\sigma \in$] 1 ; 2.5] when the VL crosses 2 switches;
- $\sigma \in$] 2.5 ; 5] when the VL crosses 3 switches.

Under the assumption of a frame is emitted every BAG_i on each VL_i (where i represents the i^{th} VL), a drawing $|N(0, \sigma_i^2)|$ has to be performed on all VL_i at a BAG_i-period to simulate the frames arrival. It results that a realistic simulation of the input flow implies a great number of Gaussian distribution-based drawings.

The mathematical expression given by the Eq. 1 cannot be directly implemented as an algorithm because of the high time cost to realize one single drawing. For many drawings, the time cost linearly grows and then, large simulations become infeasible. To address this issue, we use an approximation of the Gaussian distribution which is the algorithm of Box-Muller [12]. The algorithm of Box-Muller returns a number X following a Gaussian distribution $N(0, 1)$, and it can be expressed as follow:

$$X = \sqrt{-2\ln(U_1)} \times \cos(2\pi.U_2) \quad (2)$$

where the random variables U_1 and U_2 follow an Uniform distribution $U(0, 1)$.

From X, the relation $Y = \mu + \sigma X$ provides a value Y which follows a Gaussian distribution $N(\mu, \sigma^2)$. In the AFDX context, Y represents the frame arrival date regarding to *Tmin*.

2) Relative Frames Positions and Detection of SBFs: As AFDX network is globally asynchronous, the ES source start to transmit frames at different dates. Accordingly, the reference dates of the VLs are not the same. We call this phenomenon the *relative frames position* and we characterize it in the following.

We define $Tmin_{i,j}$ as the j^{th} date $Tmin$ of the i^{th} VL belonging to the CTRES. Fig. 3 illustrates the placement of $Tmin_{i,j}$ dates for each BAG_i for two VLs: VL_1 and VL_2. To set the relative position of $Tmin_{i,j}$, the date $Tmin_{i,1}$ is drawn according to a Uniform distribution $U(0, BAG_i)$ on the interval $[0, BAG_i]$. Once all the initial dates are set, a pattern (defined as the *hyper-period* of the input flow) repeats itself each BAG_{max} (the *maximal* BAG of the CTRES under study, since the BAG parameter is defined by a power of 2).

Thereafter, we define a *draw* as a set of initial dates $Tmin_{i,1}$ for each VL, and the frames corresponding to 20 hyper-periods. We consider that 20 hyper-periods provide a representative sample of frames and SBFs which can occur with the initial placement of $Tmin_{i,1}$.

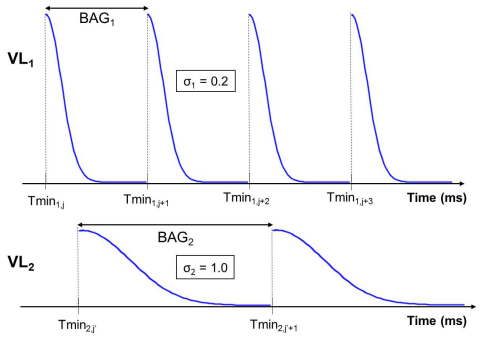

Fig. 3: Probabilistic Model applied to Two VLs with Different Relative Frames Positions of $Tmin_{i,j}$ and their associated Values σ_1 and σ_2.

However, the VL-individual frames placements with no consideration to the arrival dates and the reception durations of the other frames may lead to overlaps between frames of

different VLs. Since the VLs of the CTRES use a single physical link to reach the ES in reception, only one frame can be received at a time. To fix this issue, we draw frames in the arrival order with the Gaussian distribution-based algorithm. Then, if the current drawn frame overlaps with another one (not necessary the previous one), a tight offset is applied to ensure the minimal time duration between two consecutive frames on the physical link as specified in the ARINC 664 [1] while not impacting the Gaussian distribution.

Furthermore, the frames have no strictly periodical $Tmin_{i,j}$ dates in a real network because we generally observe a time skew during the network operations. The relative frames positions change after a certain amount of time, whatever the initial sending of frames on VLs. Thereby, we realize between 1,000 and 10,000 drawings, and we randomly replace the $Tmin_{i,j}$ dates for each drawing. As the last step, the algorithm returns the length of all SBFs and their occurrences. Each simulation generates several millions of frames, which represents 20 minutes of AFDX frames reception.

C. Characterization of the CTRES with the Link Load

To link the SBFs and the associated probabilities obtained with the Gaussian distribution-based model to the set of CTRES parameters, it is required to dispose of metrics like the link load to characterize the CTRES. We first define the link load from the CTRES parameters and the network speed, then we assess the influence of these parameters on the load value.

1) Link Load Definition: The SBFs can strongly vary from one CTRES to another depending on the number of VLs, their associated BAGs and their Maximal Frame Length (MFL). The physical link load is helpful to represent the amount of data transiting from the final switch to the reception ES. More precisely, the load is defined as the time rate during which frames are received compared to the communication medium is free. The load has a constant value as the CTRES is statically defined and is written:

$$Load = \frac{\sum_{i=1}^{\text{Number of VLs}} \frac{BAG_{max}}{BAG_i} \times L_{i,max} \times C}{BAG_{max}} \quad (3)$$

where :

- BAG_{max} is the maximum BAG value, in ms;
- $L_{i,max}$ is the MFL of the i^{th} VL, in bytes;
- C is the network speed set 12.5 bytes/s.

Thus, we distinguish *four* levels of link load:

- less than 10% - light load;
- between 10% and 20% - moderate load;
- between 20% and 40% - heavy load;
- more than 40% - very heavy load.

Last, we point out that the deterministic property cannot be ensured when the link load excess a certain threshold due to the technological limitation of switches. However, this aspect is out of the scope of this paper, and we will consider very heavy loads as theoretical examples.

2) Influence of the BAG and the MFLs on the Link Load: According to Eq. 3, the lower are the BAG_i and the higher are the $L_{i,max}$, the higher is the link load. In this part, we use a typical CTRES from [7]. For this CTRES, the initial link load is 15% for 50 VLs. This initial link load is compared to the loads obtained after variations of the MFL and the BAG parameters. In Tab. I, we present some results of the link load under a variation of the MFL of all VLs without modifying the associated BAG.

TABLE I: The Link Load under MFL Variations

Value of L_{max}, in bytes	Link Load
80	2.24%
400	11.20%
800	22.40%
1500	42.00%

As the same manner, the $L_{i,max}$ are set to their initial value, and the BAG_i are modified. All the BAG_i are first set to 2.0 ms, and then to 128 ms. Tab. II gathers the obtained results.

TABLE II: The Link Load under BAG Variations

Value of BAG, in ms	Link Load
2	61.50%
8	15.37%
32	3.84%
128	0.96%

As expected, the BAG and the MFL have a significant impact on the link load. Finally, if we combine their effect, the link load can reach 300% for 50 VLs with all BAGs set to 2.0 ms and the associated MFL set to 1,500 bytes.

IV. Simulation Results

Through a large number of simulations based on our model previously introduced, we propose to quantify the influence of CTRES parameters on the SBFs at the reception ES using the link load definition. Finally, a comparative study with a deterministic model [7] is presented.

A. Constant Link Load & Variable σ

For a given CTRES and according to Fig. 1, the VLs can pass through one or several switches, and we explained the impact of the number of passed through switches on the σ_i parameter. To study the influence of σ_i on the LSBF, we define the Lengthy VLs (L-VLs) and Curtailed VLs (C-VLs). The C-VLs pass through only 1 switch while the L-VLs pass through 2 or 3 switches. For instance, the VLs which follow the physical path $P_{1,5} = \{ES_1, Sw_1, Sw_3, Sw_5, ES_9\}$ are considered as L-VLs with 3 switches. Thus, the associated σ belongs to the interval $]\,2.5\,;\,5\,]$.

Tab. III summarizes the obtained results. We observe that the σ-distribution does not significantly impact the LSBF with a fixed load of 15%. Thereby, the number of switches that a VL passes through is not a very influential factor of the resulting LSBF when the link load is moderate.

TABLE III: The LSBF with different σ-distributions.

C-VLs	L-VLs	LSBF
90%	10%	10
50%	50%	11
10%	90%	12

B. Variable Link Loads & Different σ-Distributions

Now, we study the influence of σ-distributions with variable loads. Two types of configurations are used: one with a majority of C-VLs and the other with a majority of L-VLs, as previously define. To observe relevant results, we work with the constant number of 50 VLs using the same CTRES. The link load is modified by setting the associations of $L_{i,max}$ and BAG_i.

The three histograms referenced as Fig. 4, 5 and 6 respectively show the SBFs obtained for a rising link load of 5%, 15% and 29%.

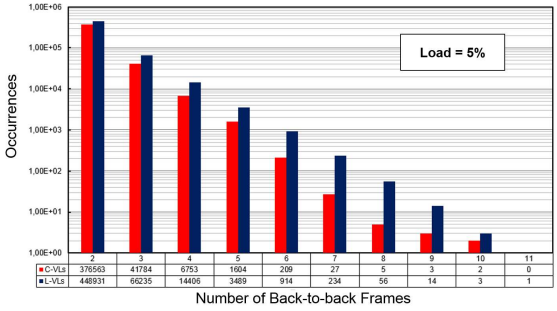

Fig. 4: Comparison of the influence of a majority of C-VLs and L-VLs for a 5% Link Load.

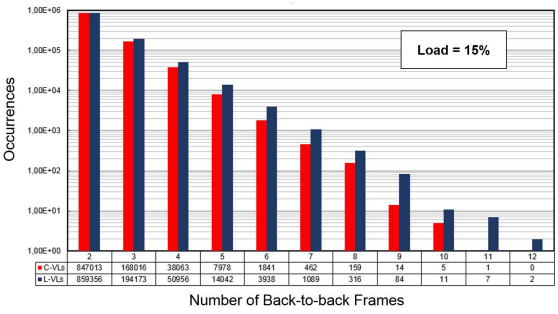

Fig. 5: Comparison of the influence of a majority of C-VLs and L-VLs for a 15% Link Load.

First, we notice that the σ-distributions have an impact on the occurrences of SFBs: the CTRESs with a majority of L-VLs imply more resulting SFBs. Tab. IV indicates the percentage of frames belonging to SBFs regarding on the CTRES under consideration.

On Fig. 4, 5 and 6, we also observe a light increase of the LSBF due to the σ-distribution when the rise of the link load. The higher is the load, the higher is the influence of the σ-distribution on the LSBF.

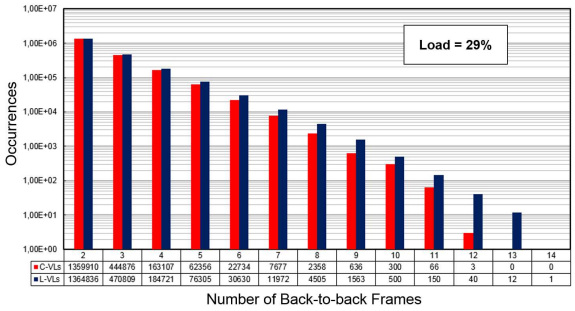

Fig. 6: Comparison of the influence of a majority of C-VLs and L-VLs for a 29% Link Load.

TABLE IV: Frames Rate belonging to SBFs for a CTRES with C-VLs & L-VLs and 50 VLs.

Load	C-VLs	L-VLs
5%	4.8%	5.9%
15%	11.9%	12.5%
29%	17.4%	18.1%

Furthermore, on Fig. 4, the influence of σ is more pronounced on short SBFs when the link is lightly loaded. In the same way, its influence is more pronounced on the medium SBFs when the link load is moderate (Fig. 5), and again more pronounced on the long SBFs when the link load is heavy (Fig. 6). Thus, we note that the influence of σ shifts according to the link load. So, if the link load between the final switch and the ES becomes heavy, the number of switches of the physical path followed by the VL has more effects on the SBFs.

C. Deterministic Model vs Probabilistic Model

Finally, we compare the results obtained with the probabilistic model to the results obtained with a deterministic model. To ensure a relevant comparison, we only use CTRESs with a mean BAG of 50.1 ms for a variance of 43.9 and a mean MFL of 307 bytes for a variance of 317.8 to be compatible with the results presented in [7]. The simulations include some dozens of millions of frames representing about 1 hour of normal network operation. The evolution of the link load associated to these CTRESs, and the LSBFs as a function of a number of VLs is shown on Fig. 7.

The deterministic model is based on a worst-case method to determine the LSBF for a given CTRES. It is used to compute the WFB, and then the minimum size of the ES reception buffer. The probabilistic model provides the probabilities of a such maximal LSBF occurs in the input flow of the ES during the network operation. Thus, it is possible to estimate the relevance of the deterministic model-based LSBF.

Fig. 7 shows that the LSBFs of the probabilistic model stay under the worst-case values and this, whatever the number of VLs. For less than 10 VLs, the results are closed. However,

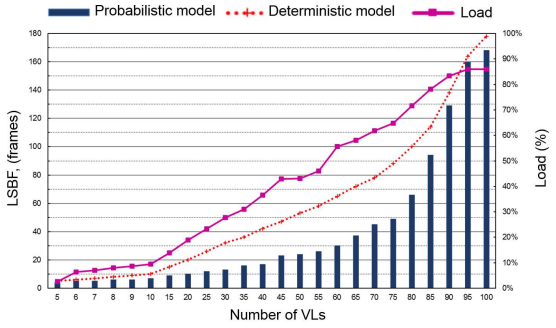

Fig. 7: Comparison of the results obtain deterministically and probabilistically.

TABLE V: Probability of the LSBF Occurrences for a Simulation Length of Several Millions of Frames.

Number of VLs	LSBF	Occurrence Probability
5	4	1.20E-04
7	5	2.53E-05
10	7	1.07E-06
15	9	3.27E-08
20	10	1.79E-06
25	12	3.73E-06
30	13	1.63E-07
35	16	2.97E-06
40	17	4.82E-06
45	23	2.11E-07
50	24	4.13E-06
55	26	3.34E-06
60	30	8.17E-08
65	37	1.57E-06
70	45	7.42E-08
75	49	3.05E-06
80	66	6.35E-08
85	94	5.77E-08
90	129	3.27E-07
95	160	1.01E-06
100	168	5.58E-08

above 85 VLs, the link load is closed to 80%. So, after this limit, the analysis becomes only theoretical. At last, between 10 and 80 VLs, a clear gap appears between the deterministic bounds and the LSBFs founded with the probabilistic model. In this region, it could be interesting to measure the occurrence probability of the probabilistic model-based LSBF.

Thus, Tab. V provides the probabilities of LSBF occurrences. Between 10 and 80 VLs, the probability of the LSBF given with the probabilistic model is inferior to 10^{-6}, and the probabilistic model-based LSBF reaches only 50% of the deterministic model-based LSBF in terms of number of frames. This could be exploited in future works to reduce the ES reception buffer.

V. Conclusion and Perspectives

An appropriate assessment of the Longest Sequence of Back-to-back Frames is necessary to correctly compute the worst frame backlog leading to the computation of the optimal ES reception buffer size.

In this paper, we presented a Gaussian distribution-based model adapted to the AFDX network constraints in order to determine the LSBF and its occurrence probabilities. We also characterized the CTRES with the link load, and we proposed a detailed analysis of the influence of CTRES parameters variations on the SBFs and on the LSBF. Finally, we proposed a comparative study between our probabilistic model and a deterministic one.

In future works, the obtained results could be useful to optimize the ES reception buffer size by addressing the relevance of the deterministic model-based LNPS. As the occurrence probability of certain LNPSs are very low (inferior to 10^{-8}), the ES reception buffer could be reduced while ensuring with the non-loss of frames.

References

[1] A. E. E. Committee, *ARINC specification 664P7: Aircraft Data Network, part 7: Avionics Full-Duplex Switched Ethernet (AFDX) network*. Aeronautical Radio Inc., June 2005.

[2] A. E. E. Committee, *ARINC specification 429: Mark 33 Digital Information Transfer System (DITS)*. Aeronautical Radio Inc., December 2004.

[3] A. E. E. Committee, *ARINC specification 419: Digital Data System Compendium*. Aeronautical Radio Inc., 1966.

[4] J. Y. LeBoudec, "Application of network calculus to guaranteed service networks," *IEEE Transactions on Information Theory*, pp. 1087–1096, 1998.

[5] H. Bauer, J. L. Scharbarg, and C. Fraboul, "Worst-case end-to-end delay analysis of an avionics afdx network," *Design, Automation & Test in Europe Conference & Exhibition (DATE)*, pp. 1220–1224, 2010.

[6] G. Kemayo, N. Benammar, F. Ridouard, H. Bauer, and P. Richard, "Improving afdx end-to-end delays analysis," *2015 IEEE 20th Conference on Emerging Technologies & Factory Automation (ETFA)*, pp. 1–8, Sept 2015.

[7] Y. Baga, F. Ghaffari, E. Zante, M. Nahmiyace, and D. Declercq, "Worst frame backlog estimation in an avionics full-duplex switched ethernet end-system," in *2016 IEEE/AIAA 35th Digital Avionics Systems Conference (DASC)*, pp. 1–10, Sept 2016.

[8] L. Ding, D. Song, X. Zeng, and Q. Hu, "The research of afdx system simulation model," *2010 International Conference on Multimedia Technology*, pp. 1–4, Oct 2010.

[9] Y. Ren, F. Hu, and J. Li, "End to end jitter control on afdx network," *Proceedings 2011 International Conference on Transportation, Mechanical, and Electrical Engineering (TMEE)*, pp. 515–518, Dec 2011.

[10] R. Mancuso, A. V. Louis, and M. Caccamo, "Using traffic phase shifting to improve afdx link utilization," *2015 International Conference on Embedded Software (EMSOFT)*, pp. 256–265, Oct 2015.

[11] B. Annighoefer, C. Reif, and F. Thieleck, "Network topology optimization for distributed integrated modular avionics," *2014 IEEE/AIAA 33rd Digital Avionics Systems Conference (DASC)*, pp. 4A1–1–4A1–12, Oct 2014.

[12] G. E. P. Box and M. E. Muller, *A Note on the Generation of Random Normal Deviates*. Ann. Math. Statist. 29, 1958.